Spectral Domain Analysis of Gyrotropic Anisotropy Chiral Effect on the Input Impedance of a Printed Dipole Antenna

Djamel Sayad[1], Fatiha Benabdelaziz[2], Chemseddine Zebiri[3], Samiha Daoudi[2], and Raed A. Abd-Alhameed[4, *]

Abstract—A theoretical analysis of a printed dipole antenna on a gyrotropic-anisotropy chiral dielectric substrate is presented. The study is based on numerical techniques for the characterization of electromagnetic propagation in chiral media. The general complex wave equation and the dispersion relation for such a medium are derived in the spectral domain. The spectral Green's function of a grounded dielectric chiral slab is developed, and the spectral domain moment method impedance matrix elements are calculated. The effect of the chiral gyrotropy element on the input impedance of a dipole antenna printed on a grounded chiral substrate is analyzed using the Galerkin-based Method of Moments.

1. INTRODUCTION

Dipole antenna designs play a crucial role in communication links for various applications; they meet the ever-growing needs of communication systems with regard to simplicity of configuration, lightness and easy integration with Monolithic Microwave Integrated Circuits (MMICs) [1]. Different shapes of dipole antennas have been analyzed over the past few decades, namely for Antenna Printed Circuits (APC) technology applications.

In recent years, there has been considerable research interest in complex media. Many theoretical and application works have been carried out on special media such as anisotropic [2], bianisotropic [3, 4] metamaterial [5, 6] and chiral materials [7–9] which have attracted much interest and support from researchers and industrials as powerful elements with a real future in microwave engineering; this is because of their many potential applications in a large number of practical problems in electromagnetic optic and acoustic domains. In particular, the work on waveguides, microstrip antennas, resonators, polarization transformers, fibers optics, microwave absorbers, and chiral-based applications have been developed in [10, 19]. Experimental works concerned with the retrieval of the effective constitutive parameters of chiral materials have been investigated as well in [3, 20, 21]. The characterization of single and multilayer printed dipole antenna structures in the presence of anisotropic permittivity material has previously been studied and analyzed in [22–24]. The Method of Moments applying the spectral domain has found to be a powerful numerical technique to solve integral equations [25]. In addition, it has been widely used in analyzing microwave planar structures over several years [26–31].

In this work, the wave equation for electromagnetic field propagation in a bounded chiral medium [32] characterized by a magnetoelectric parameters tensors is derived. The appropriate spectral Green's functions are rigorously developed. The spectral domain moment-method impedance matrix [33, 34] is used to analyze the gyrotropic anisotropy chiral dipole with arbitrary length. The impedance matrix elements are partially calculated with the aid of the numerical asymptotic

technique [35] to reduce computation time. In particular, the effect of the chirality parameter on the input impedance of the printed dipole is investigated for various dielectric properties.

2. ANALYTICAL FORMULATION

The constitutive relations for a bianisotropic medium may be written as [7]:

$$\vec{B} = \bar{\bar{\mu}}\vec{H} + \frac{\bar{\bar{\xi}}}{c}\vec{E} \tag{1a}$$

$$\vec{D} = \bar{\bar{\varepsilon}}\vec{E} + \frac{\bar{\bar{\eta}}}{c}\vec{H} \tag{1b}$$

where c is the speed of light in the free space; the 3×3 tensors $[\bar{\bar{\varepsilon}}]$ and $[\bar{\bar{\mu}}]$ are the tensors of the permittivity and permeability; $[\bar{\bar{\xi}}]$ and $[\bar{\bar{\eta}}]$ describe the cross-coupling between the electric and magnetic fields, and they are generally referred to as magnetoelectric tensors.

Equations (1a) and (1b) are valid for the constitutive description of anisotropic, biisotropic chiral, uniaxially, or biaxially bianisotropic media [36, 37].

It is assumed that the time dependence of the field to be $e^{j\omega t}$ is applied. From the general bianisotropic constitutive relations (1) and the source-free Maxwell equations, one can write the following:

$$\vec{\nabla} \times \vec{E} = -j\omega\bar{\bar{\mu}}\vec{H} - j\kappa_0\bar{\bar{\xi}}\vec{E} \tag{2a}$$

$$\vec{\nabla} \times \vec{H} = j\omega\bar{\bar{\varepsilon}}\vec{E} + j\kappa_0\bar{\bar{\eta}}\vec{H} \tag{2b}$$

where the permeability, permittivity and magnetoelectric tensors of a bianisotropic chiral medium are given respectively by [7, 32].

$$\bar{\bar{\mu}} = \begin{bmatrix} \mu_t & 0 & 0 \\ 0 & \mu_t & 0 \\ 0 & 0 & \mu_z \end{bmatrix}, \quad \bar{\bar{\varepsilon}} = \begin{bmatrix} \varepsilon_t & 0 & 0 \\ 0 & \varepsilon_t & 0 \\ 0 & 0 & \varepsilon_z \end{bmatrix} \quad \text{and} \quad \bar{\bar{\xi}} = \bar{\bar{\eta}} = j \begin{bmatrix} 0 & \xi & 0 \\ -\xi & 0 & 0 \\ 0 & 0 & 0 \end{bmatrix} \tag{3}$$

Consider the basic geometry shown in Fig. 1, which consists of a conducting patch printed along x-direction on a grounded chiral substrate of thickness d extending infinitely in the x- and y-directions, and the z-direction is normal to the patch.
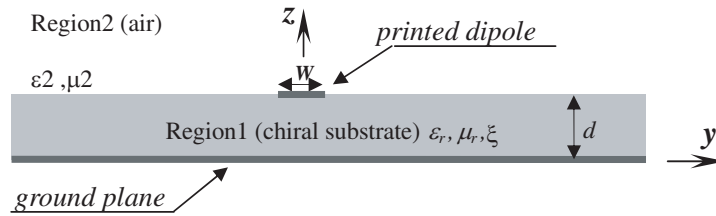

Figure 1. Cross section of the printed dipole.

Under these geometry conditions, the spectral longitudinal electromagnetic field components $\tilde{E}_z$ and $\tilde{H}_z$ are decoupled and satisfy the same wave equation; thus the 2nd order homogenous differential equation can be given by:

$$\frac{\partial^2 \tilde{E}_z}{\partial z^2} - \kappa_{ze}^2 \tilde{E}_z = 0 \tag{4a}$$

$$\frac{\partial^2 \tilde{H}_z}{\partial z^2} - \kappa_{zh}^2 \tilde{H}_z = 0 \tag{4b}$$

where

$$\kappa_{ze}^2 = \kappa_0^2 \left(\varepsilon_t \mu_t - \xi^2 \right) - \frac{\varepsilon_t}{\varepsilon_z}\kappa_s^2 \tag{5a}$$

$$\kappa_{zh}^2 = \kappa_0^2 \left(\varepsilon_t \mu_t - \xi^2 \right) - \frac{\mu_t}{\mu_z} \kappa_s^2 \tag{5b}$$

And

$$\kappa_s^2 = \kappa_x^2 + \kappa_y^2 \tag{6}$$

κ_{ze} and κ_{zh} represent the dispersion relations for TM and TE modes, respectively. κ_0 is the free space wave number.

3. METHOD OF SOLUTION

Now, solving for the spectral components $\tilde{E}_z$ and $\tilde{H}_z$ in region 1 within the dielectric, these can be expressed by:

$$\tilde{E}_{z1} = a_e e^{j\kappa_{ze}z} + b_e e^{-j\kappa_{ze}z} \tag{7a}$$

$$\tilde{H}_{z1} = a_h e^{j\kappa_{zh}z} + b_h e^{-j\kappa_{zh}z} \tag{7b}$$

On the other hand, at region 2 above the patch (i.e., the air medium), the spectral components are decaying waves with z, in which the following solutions are assumed:

$$\tilde{E}_{z2} = a_1 e^{-j\kappa_2(z-d)} \tag{8a}$$

$$\tilde{H}_{z2} = a_2 e^{-j\kappa_2(z-d)} \tag{8b}$$

$$\kappa_2^2 = \omega^2 \mu_0 \varepsilon_0 - \kappa_s^2 \tag{9}$$

It should be noted that all the transverse components of the electromagnetic field are expressed in terms of the longitudinal components $\tilde{E}_z$ and $\tilde{H}_z$ in both regions.

The complex constants appearing in these expressions of the electromagnetic field components are determined using the appropriate boundary conditions.

3.1. Derivation of the Green's Functions

The enforcement of the tangential boundary conditions at the interface containing the printed patch between the two regions leads to extensive algebraic manipulations. At $z = d$ it results:

$$\tilde{E}_{x1} = \tilde{E}_{x2} \tag{10a}$$

$$\tilde{E}_{y1} = \tilde{E}_{y2} \tag{10b}$$

$$\tilde{H}_{y2} - \tilde{H}_{y1} = \tilde{J}_x \tag{10c}$$

$$\tilde{H}_{x1} - \tilde{H}_{x2} = \tilde{J}_y \tag{10d}$$

The resulting mathematical equations lead to the expressions of the tangential components of the electric field $\tilde{E}_x$ and $\tilde{E}_y$ evaluated at the interface between the two media with respect to the current densities $J_x(x,y)$ and $J_y(x,y)$. Consequently, the spectral Green's tensor elements are determined according to the following system of equations, evaluated at $z = d$.

$$\tilde{E}_x = \tilde{G}_{xx} \tilde{J}_x + \tilde{G}_{xy} \tilde{J}_y \tag{11a}$$

$$\tilde{E}_y = \tilde{G}_{yx} \tilde{J}_x + \tilde{G}_{yy} \tilde{J}_y \tag{11b}$$

where $\tilde{J}_x$ and $\tilde{J}_y$ are the Fourier transforms of the current densities on the patch, according to the configuration in Fig. 1.

In narrow dipole configuration analysis, the structure of interest, the transverse current density in the y-direction is generally neglected, because the width of the strip is assumed to be very small. Therefore, only the Green's function $\tilde{G}_{xx}$, in Equation (11), is developed herein, and the other functions will not be presented in this work, since they are not involved in the calculations. Equation (12) gives the expression of $\tilde{G}_{xx}$ at $z = d$, for the chiral medium.

$$\tilde{G}_{xx}(\kappa_s) = -\frac{jZ_0}{\kappa_0} \left[\frac{\kappa_z \kappa_x^2 \left(\kappa_0^2 \varepsilon_r \mu_r - \kappa_s^2 \right)}{\kappa_s^2 \, T_m} + \frac{\kappa_y^2 \kappa_0^2 \mu_r}{\kappa_s^2 \, T_e} \right] \sin(\kappa_{1z} d) \tag{12}$$

with

$$T_m = \kappa_{1z}\kappa_z\varepsilon_r \cos\left(\kappa_{1z}d\right) + j\left(\kappa_0^2\varepsilon_r\mu_r - \kappa_s^2 - j\kappa_z\kappa_0\xi\varepsilon_r\right)\sin\left(\kappa_{1z}d\right) \tag{13}$$

$$T_e = \kappa_{1z}\cos\left(\kappa_{1z}d\right) + j\left(\kappa_z\mu_r - j\kappa_0\xi\right)\sin\left(\kappa_{1z}d\right) \tag{14}$$

$$\kappa_{1z}^2 = \kappa_0^2\left(\varepsilon_r\mu_r - \xi^2\right) - \kappa_s^2, \quad \mathrm{Im}\left(\kappa_{1z}\right) < 0$$

$$\kappa_z^2 = \kappa_0^2 - \kappa_s^2, \quad \mathrm{Im}\left(\kappa_z\right) < 0$$

where Z_0 is the free space impedance.

By setting the relative permeability $\mu_r = 1$ and the chirality element $\xi = 0$ in Equation (12), with further rearrangement of the $\tilde{G}_{xx}$ expression, one can get the same isotropic-case $\tilde{G}_{xx}$ expression given in [33, 38–40].

4. NUMERICAL RESULTS

In microstrip planar structures and printed dipole antennas, the spectral domain moment method impedance matrix elements can be expressed by the following double integral equation [34, 35, 41]:

$$\tilde{Z}_{mn} = -\frac{1}{4\pi^2}\int\limits_{-\infty}^{\infty}\int\limits_{-\infty}^{\infty}\tilde{J}_m\left(\kappa_x,\kappa_y\right)\tilde{G}\left(\kappa_x,\kappa_y\right)\tilde{J}_n^*\left(\kappa_x,\kappa_y\right)d\kappa_x d\kappa_y \tag{15}$$

To solve the above equation the test functions are assumed equal to the basis functions, thus Galerkin's solution is assumed.

4.1. Evaluation of the Input Impedance

The effect of the bi-isotropic chiral substrate on the input impedance is considered here. In order to validate calculations, it has initially considered the isotropic case ($\mu_r = 1$ and $\xi = 0$ in Equation (12)). Fig. 2 presents the input impedance (real and imaginary parts) of a planar dipole of width $W = 0.01\lambda_0$ as a function of the normalized length L/λ_0. The dipole is printed on an isotropic grounded dielectric slab of thickness $d = 0.0796\lambda_0$ and dielectric constant $\varepsilon_r = 3.25$. The results are compared with [35] and show reasonable agreements.
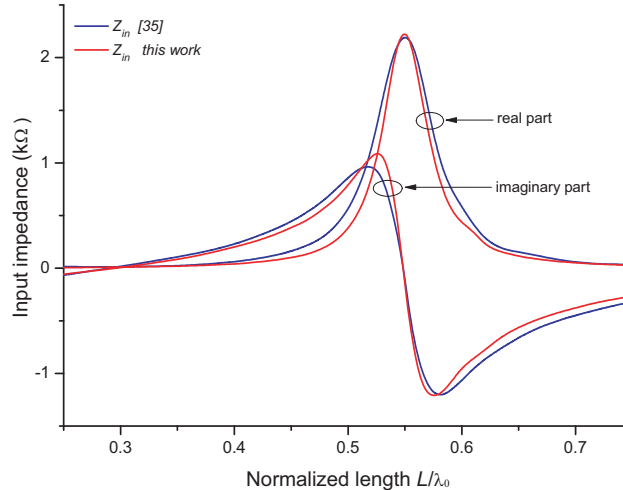

Figure 2. Real and imaginary parts of input impedance of isotropic printed dipole antenna, $W = 0.01\lambda_0$, $d = 0.0796\lambda_0$ and $\varepsilon_r = 3.25$.

Two resonant lengths can be observed corresponding to two points where the input impedance is purely real. The first is located at $0.295\lambda_0$ and the second at $0.55\lambda_0$. These resonant lengths correspond to the effective half and full wavelengths of the printed dipole antenna, respectively.
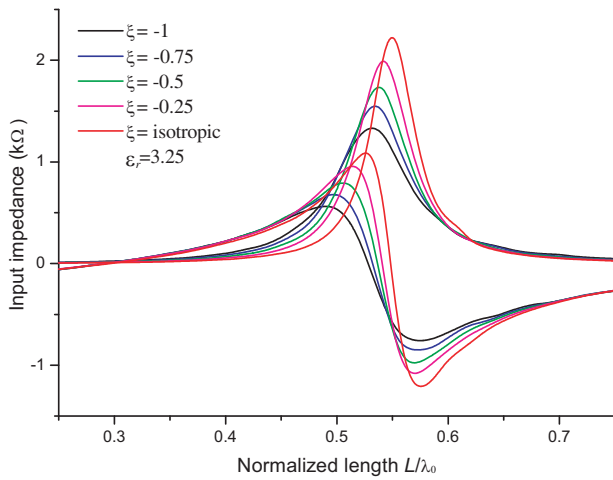
Figure 3. Negative-chirality effect on the input impedance of bi-isotropic chiral dipole antenna, $W = 0.01\lambda_0$, $d = 0.0796\lambda_0$ and $\varepsilon_r = 3.25$.
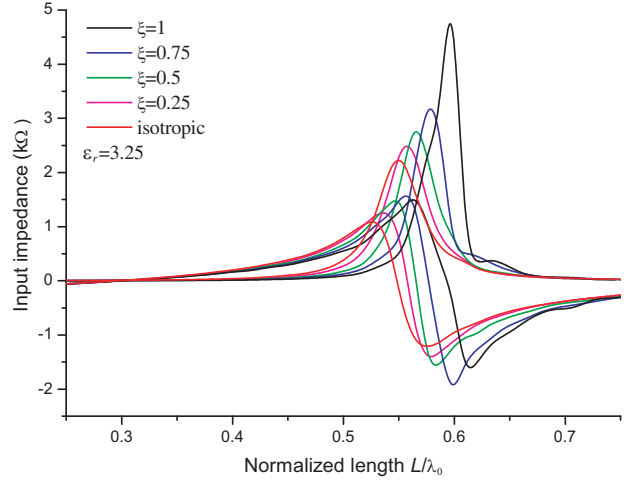

Figure 4. Positive-chirality effect on the input impedance of bi-isotropic chiral dipole antenna, $W = 0.01\lambda_0$, $d = 0.0796\lambda_0$ and $\varepsilon_r = 3.25$.

Figure 5. Negative-chirality effect on the input impedance of bi-isotropic chiral dipole antenna, $W = 0.01\lambda_0$, $d = 0.0796\lambda_0$ and $\varepsilon_r = 2.5$.

Figure 6. Positive-chirality effect on the input impedance of bi-isotropic chiral dipole antenna, $W = 0.01\lambda_0$, $d = 0.0796\lambda_0$ and $\varepsilon_r = 2.5$.
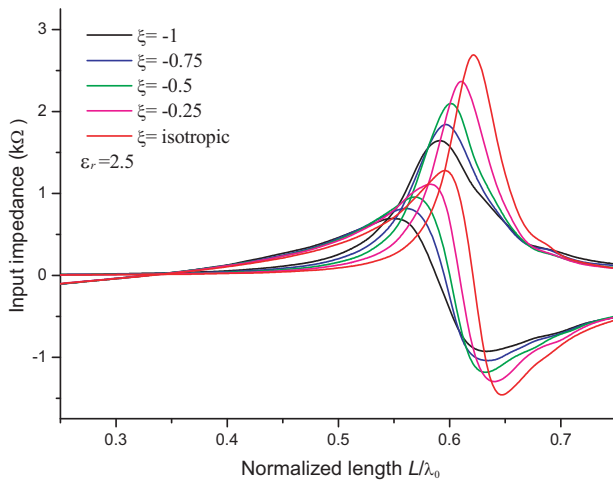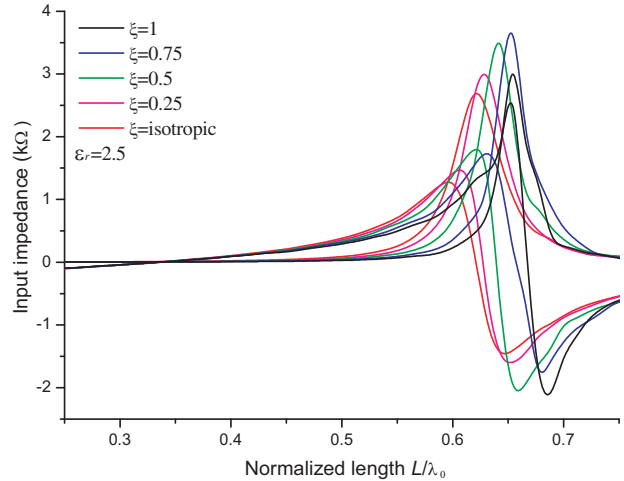
Figures 3 and 4 show the variations of the real and imaginary parts of the input impedance of a chiral dipole antenna for various negative and positive values of ξ respectively with a permittivity of $\varepsilon_r = 3.25$ compared with the isotropic case. It can be seen that the two resonance points shift left with negative chirality values as in Fig. 3, whereas they shift right with positive chirality ones as in Fig. 4. The latter case may help to enhance the impedance bandwidth around the first resonance since the variation in the impedance amplitude in this region is very slow. It is easy to observe that the chirality has a direct effect on the amplitude of the input impedance that increases with increasing ξ mainly round the second resonance region (Figs. 3, 4, 5 and 6).

It is worth noting that the effect of chirality on the input impedance characteristics is more significant for lower values of relative permittivities as shown in Figs. 5 and 6.

Figures 7 and 8 present respectively the effect of chirality on the half and full wavelength resonance for various dielectric constants ε_r. It can be seen that the second resonance is more affected by the chirality, and large shift in resonances occurs in the case of lower permittivity dielectrics when ε_r values are closer to ξ.
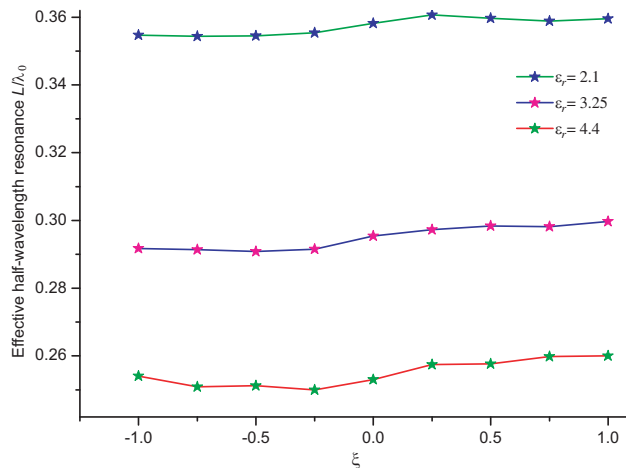
Figure 7. Effect of chirality on half-wavelength resonance for various dielectric constants ε_r.
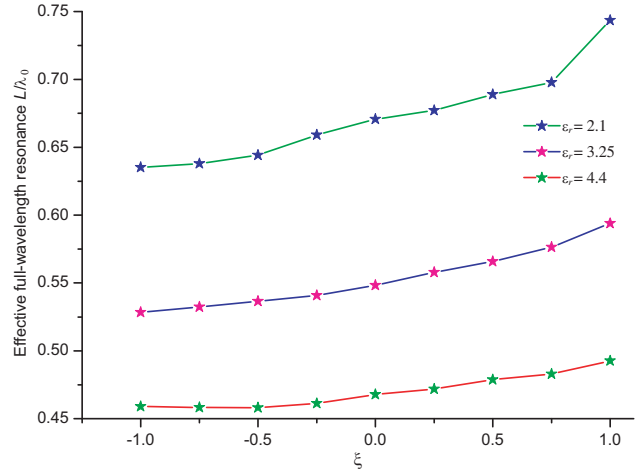

Figure 8. Effect of chirality on full-wavelength resonance for various dielectric constants ε_r.

5. CONCLUSIONS

In this work, a theoretical study of the chirality effect on the input impedance and resonance lengths of a dipole antenna is presented using the spectral domain moment method based on the rigorous derivation of the appropriate Green's function. The introduction of the chirality in the dielectric slab significantly affects the dipole input impedance in terms of resonance length and amplitude. The results show a significant shift at the half and the one wavelength resonances, in particular with lower dielectric constants of the media. It is concluded that the chirality constitutes an additional parameter that can be used to control the input impedance and to enhance bandwidth improvement including the miniaturization of the dipole antenna by designing a specific resonant length for a given dipole application.

REFERENCES

1. Kim, M. J., C. S. Cho, and J. Kim, "A dual band printed dipole antenna with spiral structure for WLAN application," *IEEE Microwave and Wireless Components Letters*, Vol. 15, No. 12, 910–912, Dec. 2005.

2. Wu, J. and K. Sarabandi, "Anisotropic magneto-dielectrics for wideband planar antenna miniaturization applications," *2014 USNC-URSI Radio Science Meeting (Joint with AP-S Symposium)*, 111–111, Memphis, TN, 2014.

3. Zarifi, D., M. Soleimani, and A. Abdolali, "Electromagnetic characterization of biaxial bianisotropic media using the state space approach," *IEEE Transactions on Antennas and Propagation*, Vol. 62, No. 3, 1538–1542, Mar. 2014.

4. Havrilla, M. J., "Scalar potential formulation for a bianisotropic gyrotropic inhomogeneous medium and associated boundary conditions," *2014 USNC-URSI Radio Science Meeting (Joint with AP-S Symposium)*, 162–162, Memphis, TN, 2014.

5. Jamilan, S., M. A. Antoniades, J. Nourinia, and M. N. Azarmanesh, "A compact multiband printed dipole antenna loaded with two unequal parallel NRI-TL metamaterial unit cells," *IEEE Transactions on Antennas and Propagation*, Vol. 63, No. 9, 4244–4250, Sep. 2015.

6. Islam, M. M., M. T. Islam, M. Samsuzzaman, and M. R. I. Faruque, "Compact metamaterial antenna for UWB applications," *Electronics Letters*, Vol. 51, No. 16, 1222–1224, 2015.

7. Bilotti, F. and L. Vegni, "Chiral cover effects on microstrip antennas," *IEEE Transactions on Antennas and Propagation*, Vol. 51, No. 10, 2891–2898, Oct. 2003.

8. Zebiri, C., M. Lashab, and F. Benabdelaziz, "Rectangular microstrip antenna with uniaxial bi-anisotropic chiral substrate-superstrate," *IET Microwaves, Antennas & Propagation*, Vol. 5, No. 1, 17–29, 2011.

9. Ouchetto, B. A. El Majd, H. Ouchetto, B. Essakhi, and S. Zouhdi, "Homogenization of periodic structured materials with chiral properties," *IEEE Transactions on Antennas and Propagation*, Vol. 64, No. 5, 1751–1758, May 2016.

10. Cory, H., "Chiral devices — An overview of canonical problems" *Journal of Electromagnetic Waves and Applications*, Vol. 9, Nos. 5–6, 805–829, 1995.

11. Zebiri, C., F. Benabdelaziz, and D. Sayad, "Surface waves investigation of a bianisotropic chiral substrate resonator," *Progress In Electromagnetics Research B*, Vol. 40, 399–414, 2012.

12. Zebiri, C., M. Lashab, and F. Benabdelaziz, "Asymmetrical effects of bi-anisotropic substrate-superstrate sandwich structure on patch resonator," *Progress In Electromagnetics Research B*, Vol. 49, 319–337, 2013.

13. Hussain, A., M. Faryad, and Q. A. Naqvi, "Fractional curl operator and fractional chiro-waveguide," *Journal of Electromagnetic Waves and Applications*, Vol. 21, No. 8, 1119–1129, 2007.

14. Kopp, V. I., J. Park, M. Wlodawski, J. Singer, D. Neugroschl, and A. Z. Genack, "Chiral fibers: Microformed optical waveguides for polarization control, sensing, coupling, amplification, and switchin," *Journal of Lightwave Technology*, Vol. 32, No. 4, 605–613, 2014.

15. Ghaffar, A., M. Arif, Q.-A. Naqvi, and M.-A. Alkanhal, "Radiation properties of a uniaxial chiral quadratic inhomogeneous slab under oblique incidence," *Optik — International Journal for Light and Electron Optics*, Vol. 125, No. 4, 1589–1597, 2014.

16. Panin, S. B., P. D. Smith, and A. Y. Poyedinchuk, "Elliptical to linear polarization transformation by a grating on a chiral medium," *Journal of Electromagnetic Waves and Applications*, Vol. 21, No. 13, 1885–1899, 2007.

17. Lim, K. Y., P. K. Choudhury, and Z. Yusoff, "Chirofibers with helical windings — An analytical investigation," *Optik*, Vol. 121, No. 11, 980–987, 2010.

18. Yang, S.-K. and S.-Y. Hsia, "Chiral composites as underwater acoustic attenuators?," *IEEE Journal of Oceanic Engineering*, Vol. 25, No. 1, 139–145, 2000.

19. Cloete, J. H., M. Bingle, and D. B. Davidson, "The role of chirality and resonance in synthetic microwave absorbers," *AEU International Journal of Electronics and Communications*, 2001.

20. Bayatpur, F., A. V. Amirkhizi, and S. Nemat-Nasser, "Experimental characterization of chiral uniaxial bianisotropic composites at microwave frequencies," *IEEE Transactions on Microwave Theory and Techniques*, Vol. 60, No. 4, 1126–1135, 2012.

21. Chen, X., B. I. Wu, J. A. Kong, and T. M. Grzegorczyk, "Retrieval of the effective constitutive parameters of bianisotropic metamaterials," *Phys. Rev. E, Stat. Phys. Plasmas Fluids Relat. Interdiscip. Top.*, Vol. 71, 46610–46618, 2005.

22. Eroglu, A. and J. K. Lee, "Far field radiation from an arbitrarily orientated Hertzian dipole in the presence of layered anisotropic medium," *IEEE Transactions on Antennas and Propagation*, Vol. 53, No. 12, 3963–3973, 2005.

23. Braaten, B. D., R. M. Nelson, and D. A. Rogers, "Input impedance and resonant frequency of a printed dipole with arbitrary length embedded in stratified uniaxial anisotropic dielectrics," *IEEE Antennas Wireless Propag. Lett.*, Vol. 8, 806–810, 2009.

24. Braaten, B. D., D. A. Rogers, and R. M. Nelson, "Multi-conductor spectral domain analysis of the mutual coupling between printed dipoles embedded in stratified uniaxial anisotropic dielectrics," *IEEE Transactions on Antennas and Propagation*, Vol. 60, No. 4, 1886–1898, Apr. 2012.

25. Harrington, R. F., *Field Computation by Moment Methods*, IEEE Press, Inc., NY, 1992.

26. Di Ruscio, D., P. Burghignoli, P. Baccarelli, D. Comite, and A. Galli, "Spectral Method of Moments for planar structures with azimuthal symmetry," *IEEE Transactions on Antennas and Propagation*, Vol. 62, No. 4, 2317–2322, Apr. 2014.

27. Pozar, D. M., "Improved computational efficiency for the method of moments solution of printed dipoles and patch," *Electromagn.*, Vol. 3, 299–309, Jul.–Sep. 1983.

28. Gibson, W. C., *The Method of Moments in Electromagnetics*, Chapman & Hall/CRC, 2008.

29. Swanson, Jr., D. G. and W. J. R. Hoefer, *Microwave Circuit Modeling Using Electromagnetic Field Simulation*, Artech House, 2003.

30. Davidson, D. B. and J. T. Aberle, "An introduction to the spectral domain Method-of-Moments formulations," *IEEE Antennas Propag. Mag.*, Vol. 46, No. 3, 11–19, Jun. 2004.

31. Zang, S. R. and J. R. Bergmann, "Analysis of omnidirectional dual-reflector antenna and feeding horn using Method of Moments," *IEEE Transactions on Antennas and Propagation*, Vol. 62, No. 3, 1534–1538, Mar. 2014.

32. Zebiri, C., S. Daoudi, F. Benabdelaziz, M. Lashab, D. Sayad, N. T. Ali, and R. A. Abd-Alhameed, "Gyro-chirality effect of bianisotropic substrate on the operational of rectangular microstrip patch antenna," *International Journal of Applied Electromagnetics and Mechanics*, 1–1, 2016, Preprint.

33. Pozar, D., "Radiation and scattering from a microstrip patch on a uniaxial substrate," *IEEE Transactions on Antennas and Propagation*, Vol. 35, No. 6, 613–621, Jun. 1987.

34. Pozar, D. M., "Input impedance and mutual coupling of rectangular microstrip antennas," *IEEE Transactions on Antennas and Propagation*, Vol. 30, 1191–1196, Nov. 1982.

35. Park, S.-O. and C. A. Balanis, "Analytical technique to evaluate the asymptotic part of the impedance matrix of Sommerfeld-type integrals," *IEEE Transactions on Antennas and Propagation*, Vol. 45, No. 5, 798–805, May 1997.

36. Bilotti, F., L. Vegni, and A. Toscano, "Radiation and scattering features of patch antennas with bianisotropic substrates," *IEEE Transactions on Antennas and Propagation*, Vol. 51, No. 3, 449–456, Mar. 2003.

37. Li, L.-W. and W.-Y. Yin, "Linear complex media," *Encyclopedia of RF and Microwave Engineering*, 694–717, John Wiley, New York, 2005.

38. Li, K., S.-O. Park, H. Lee, J. Ma, B.-C. Kim, and H.-D. Choi, "Analytical technique to evaluate the asymptotic part of the impedance matrix of microstrip dipole on a uniaxial substrate," *Progress In Electromagnetics Research*, Vol. 35, 127–139, 2002.

39. Pan, G.-W., J. Tan, and J. D. Murphy, "Full-wave analysis of microstrip floating-line discontinuities," *IEEE Transactions on Electromagnetic Compatibility*, Vol. 36, No. 1, Feb. 1994.

40. Park, S.-O., C. A. Balanis, and C. R. Birtcher, "Analytical evaluation of the asymptotic impedance matrix of a grounded dielectric slab with roof-top functions," *IEEE Transactions on Antennas and Propagation*, Vol. 46, No. 2, 251–259, Feb. 1998.

41. Jackson, R. W. and D. M. Pozar, "Full-wave analysis of microstrip openend and gap discontinuities," *IEEE Transactions on Microwave Theory and Techniques*, Vol. 33, 1036–1042, Oct. 1985.